

## Original Research

A novel method for identifying SARS-CoV-2 infection mutants via an epitope-specific CD8<sup>+</sup> T cell test

Congling Qiu<sup>a,1</sup>, Bo Peng<sup>b,1</sup>, Chanchan Xiao<sup>c,d,e,1</sup>, Pengfei Chen<sup>c,1</sup>, Lipeng Mao<sup>f</sup>, Xiaolu Shi<sup>g</sup>, Zhen Zhang<sup>h</sup>, Ziquan Lv<sup>i</sup>, Qiuying Lv<sup>h</sup>, Xiaomin Zhang<sup>g</sup>, Jiaxin Li<sup>a</sup>, Yanhao Huang<sup>c</sup>, Qinghua Hu<sup>b</sup>, Guobing Chen<sup>c,d,e,\*</sup>, Xuan Zou<sup>b,\*</sup>, Xiaofeng Liang<sup>a,\*</sup>

<sup>a</sup> Department of Public Health and Preventive Medicine, School of Medicine, Jinan University, Kangtai Biological Vaccine Industry Research Institute/Disease Prevention and Control Institute of Jinan University, Guangzhou 510632, China

<sup>b</sup> Shenzhen Center for Disease Control and Prevention, Shenzhen 518020, China

<sup>c</sup> Department of Microbiology and Immunology, Institute of Geriatric Immunology, School of Medicine, Jinan University, Guangzhou 510632, China

<sup>d</sup> Key Laboratory of Viral Pathogenesis & Infection Prevention and Control (Jinan University), Ministry of Education, Guangzhou 510632, China

<sup>e</sup> The Sixth Affiliated Hospital, Jinan University, Guangzhou 510632, China

<sup>f</sup> Department of Systems Biomedical Sciences, School of Medicine, Jinan University, Guangzhou 510632, China

<sup>g</sup> Microbiology Laboratory, Shenzhen Center for Disease Control and Prevention, Shenzhen 518020, China

<sup>h</sup> Department of Communicable Diseases Control and Prevention, Shenzhen Center for Disease Control and Prevention, Shenzhen 518020, China

<sup>i</sup> Central Laboratory, Shenzhen Center for Disease Control and Prevention, Shenzhen 518020, China

## ARTICLE INFO

## Article history:

Received 16 August 2023

Revised 7 March 2024

Accepted 14 March 2024

Available online 25 March 2024

## Keywords:

Asymptomatic coronavirus disease 2019 (COVID-19)

Epitopes

Specific CD8<sup>+</sup> T cell

ELISpot

## ABSTRACT

Since the outbreak of the coronavirus disease 2019 (COVID-19) epidemic in 2019, the public health system has faced enormous challenges. Tracking the individuals who test positive for severe acute respiratory syndrome coronavirus 2 (SARS-CoV-2) is a key step for interrupting chains of transmission of SARS-CoV-2 and reducing COVID-19-associated mortality. With the increasing of asymptomatic infections, it is difficult to track asymptomatic infections through epidemiological surveys and virus whole-genome sequencing. However, due to the cross-reactivity of neutralizing antibodies produced by multiple virus subtypes, neutralizing antibody detection cannot be used to determine whether an individual has a history of infection with a specific subtype of SARS-CoV-2. We recruited 4 human leukocyte antigen A2 (HLA-A2) infections, 15 individuals who received three doses of inactivated vaccines, and 30 breakthrough infections after vaccination and discussed a case-tracking approach to detect epitope-specific CD8<sup>+</sup> T cells in the peripheral blood of close contacts, including accurate HLA typing based on ribonucleic acid (RNA)-sequencing and flow cytometry data and the comparison and characterization of SARS-CoV-2 HLA-A2 and HLA-A24 epitope-specific CD8<sup>+</sup> T cells. From individuals who received three doses of inactivated vaccine, we observed that the CD8<sup>+</sup> T cell specificity for ancestral epitopes was significantly higher than for mutated epitopes, and the fold change of CD8<sup>+</sup> T cells corresponding to mutated epitopes relative to ancestral epitopes was less than 1. The enzyme-linked immunospot (ELISpot) results further validate this result. This study forms a “method for understanding the infection history of SARS-CoV-2 subtypes based on the proportion of epitope-specific CD8<sup>+</sup> T cells in the peripheral blood of subjects”, covering up to 46 % of the population, including HLA-A2<sup>+</sup> and HLA-A24<sup>+</sup> donors, providing a novel method for SARS-CoV-2 infected case tracing.

© 2024 Chinese Medical Association Publishing House. Published by Elsevier BV. This is an open access article under the CC BY-NC-ND license (<http://creativecommons.org/licenses/by-nc-nd/4.0/>).

\* Corresponding authors: Department of Microbiology and Immunology, Institute of Geriatric Immunology, School of Medicine, Jinan University, Guangzhou 510632, China (G. Chen); Shenzhen Center for Disease Control and Prevention, Shenzhen 518020, China (X. Zhou); Department of Public Health and Preventive Medicine, School of Medicine, Jinan University, Kangtai Biological Vaccine Industry Research Institute/Disease Prevention and Control Institute of Jinan University, Guangzhou 510632, China (X. Liang).

E-mail addresses: [guobingchen@jnu.edu.cn](mailto:guobingchen@jnu.edu.cn) (G. Chen), [914494557@qq.com](mailto:914494557@qq.com) (X. Zou), [liangxf@jnu.edu.cn](mailto:liangxf@jnu.edu.cn) (X. Liang).

<sup>1</sup> These authors contributed equally to this study.

<https://doi.org/10.1016/j.bsheal.2024.03.005>

2590-0536/© 2024 Chinese Medical Association Publishing House. Published by Elsevier BV.

This is an open access article under the CC BY-NC-ND license (<http://creativecommons.org/licenses/by-nc-nd/4.0/>).

## 1. Introduction

The severe acute respiratory syndrome coronavirus 2 (SARS-CoV-2) pandemic that causes coronavirus disease 2019 (COVID-19) continues to place unprecedented pressure on the lives and economies of many countries. As countries further liberalize prevention and control policies, healthcare systems are overwhelmed by rising numbers of COVID-19 cases [1].

In response to the spread of the highly transmissible Omicron variant, the world is actively responding to the precise handling of local-

## HIGHLIGHTS

### Scientific question

Effective tracking of the coronavirus disease 2019 (COVID-19) cases is essential for controlling the disease's spread, but traditional methods struggle to identify asymptomatic carriers, creating a gap in transmission control. This highlights a pressing need for innovative strategies that is capable of more reliably detecting infections.

### Evidence before this study

Traditional tracking methods, including sequencing and antibody detection, can face significant hurdles in identifying asymptomatic infections. This is due to the complexities of cross-immunity and the often low viral loads present in such cases. In contrast, T cells offer a unique advantage due to their long-lasting memory response and the heightened sensitivity of epitope-specific T cells. These characteristics enable the detection of historical infections that might otherwise be overlooked by conventional tracking approaches.

### New findings

This study introduces a novel method for tracing the severe acute respiratory syndrome coronavirus 2 (SARS-CoV-2) infections by analyzing the proportion of epitope-specific CD8<sup>+</sup> T cells in peripheral blood, applicable to 46 % of the population, including those with positive human leukocyte antigen A2 (HLA-A2<sup>+</sup>) and positive human leukocyte antigen A24 (HLA-A24<sup>+</sup>), thereby offering a new perspective on infection tracking.

### Significance of the study

This novel detection method marks a significant step forward in epidemiology and public health, offering a more accurate and inclusive way to trace COVID-19 infections, particularly among asymptomatic individuals or where antibody responses have declined. It could lead to improved containment strategies and a better understanding of the virus's impact.

ized COVID-19 cases, quickly cutting off the chain of transmission and ending the epidemic promptly. Tracking and monitoring individuals who test positive for SARS-CoV-2 is a key step for interrupting chains of transmission of SARS-CoV-2 and reducing COVID-19-associated mortality [2]. Epidemiological investigation and emerging whole-genome sequencing (WGS) have been widely used to track and monitor individuals infected with SARS-CoV-2 [3].

With the further liberalization of the policy, the number of people undergoing nucleic acid testing has decreased, and it is impossible to obtain complete monitoring of the infected population, and many of them are asymptomatic COVID-19 patients who do not realize that they have been infected. Moreover, the virus exists in the body of asymptomatic COVID-19 patients for a short time, and it is difficult to collect the virus, which makes it impossible to trace the source of the virus through WGS [4]. Therefore, neutralizing antibody detection can solve the problem of determining whether individuals without a vaccination history are infected with SARS-CoV-2 to a certain extent when nucleic acid collection is not possible. However, in individuals with a history of vaccination, it is difficult to determine whether the subject is infected due to the cross-reactivity of neutralizing antibodies between virus mutants. Moreover, since many studies have shown that neutralizing antibodies in infected persons can last for approximately 6 months, theoretically, neutralizing antibody detection can be used

to determine whether an individual has been infected with SARS-CoV-2 within half a year [5].

In the third year of the outbreak, more than 89.7 % of the population completed the full course of vaccination against SARS-CoV-2 in China, so most of the population already has neutralizing antibodies in their bodies. Furthermore, since the neutralizing antibodies produced by multiple virus subtypes have a certain cross-reactivity, it is impossible to determine whether an individual has a history of infection with a specific subtype of SARS-CoV-2 through neutralizing antibody detection [6]. According to our previous screening of the original and mutant CD8<sup>+</sup> T-cell-specific epitopes of SARS-CoV-2, we speculate that it is possible to determine whether an individual has a history of infection by detecting mutant epitope-specific CD8<sup>+</sup> T cells [7].

## 2. Materials and methods

### 2.1. Human subject enrollment

The donors had no known history of any significant systemic diseases, including but not limited to hepatitis B or C, HIV, diabetes, kidney or liver diseases, malignant tumors, or autoimmune diseases (Tables S1–S4). All the sample information was blinded during all the experiments.

### 2.2. Isolation of plasma and PBMCs

Whole blood was collected in heparinized blood vacutainers and kept on gentle agitation until processing. Plasma specimens were collected after centrifugation of whole blood at 600 × g for 10 min at room temperature (RT) without braking. The undiluted plasma was transferred to 1.5 mL cryotubes and stored at –80 °C for subsequent analysis. Peripheral blood mononuclear cells (PBMCs) were isolated by density gradient centrifugation using a lymphocyte separation medium (GE, US). Percentage viability was estimated using standard Trypan blue staining. The PBMCs were cryopreserved in fetal bovine serum (LONSERA, Uruguay) with 10 % dimethyl sulfoxide (DMSO) (Sigma-Aldrich, US) and stored in liquid nitrogen until use.

### 2.3. RNA extraction and sequencing

Total ribonucleic acid (RNA) was isolated from PBMCs of 6 donors by using TRIzol Reagent (Invitrogen) (Table S1). RNA purity was checked by the NanoPhotometer spectrophotometer (IMPLEN), and integrity was assessed using the RNA Nano 6000 Assay Kit of the Bioanalyzer 2100 system (Agilent Technologies). Then, cDNA libraries were constructed using 0.1 µg RNA per specimen with the NEBNext Ultra™ RNA Library Prep Kit for Illumina (NEB) following the manufacturer's recommendations, and index codes were added to attribute sequences to each sample. The clustering of the index-coded samples was performed on a cBot Cluster Generation System using TruSeq PE Cluster Kit v3-cBot-HS (Illumina). After cluster generation, the library preparations were sequenced on an Illumina NovaSeq platform, and 150 bp paired-end reads were generated.

### 2.4. HLA subtype analysis of RNA-seq data

OptiType was used for classifying and identifying the RNA-seq data obtained above. First, OptiType was compared with the human reference genome to obtain chromosome 6 data from the bam file. Then, a novel human leukocyte antigen (HLA) typing algorithm based on integer linear programming was used to accurately identify HLA typing [8].

### 2.5. Human HLA subtypes were identified by flow cytometry

Donors were identified by flow antibody staining without subtype identification. Briefly, 1 × 10<sup>6</sup> PBMCs were stained with phycoery-

thrin (PE)-conjugated anti-human HLA-A2 antibody (BioLegend, Cat# 343305, US) and fluorescein isothiocyanate (FITC)-conjugated anti-human HLA-A2 antibody (MBL, Cat# K0208-4, Japan) and acquired using a flow cytometer for 30 min at 4 °C in the dark.

## 2.6. HLA-A2/A24 restricted T-cell epitope prediction

The membrane (M), envelope (E), nucleocapsid (N), open reading frame (ORF), and spike (S) protein sequences of the SARS-CoV-2 ancestral-Hu-1 strain (NC\_045512.2) were analyzed using the “Major histocompatibility complex (MHC)-I Binding” tool for CD8<sup>+</sup> T cell epitope prediction. The prediction method used was IEDB website recommendation 2.22 (<https://tools.iedb.org/mhci>) (NetMHCpan EL), and the HLA subtype selected was HLA-A\*02:01/HLA-A\*24. We predicted all CD8<sup>+</sup> T epitopes from the virus sequencing results of donor 001 (Table S5). The epitope with the best antigen presentation score was used as the candidate peptide of the ancestral strain. Epitopes from mutant strains were excluded with peptide length > 12 aa and predicted antigen presentation ability by VaxiJen 2.0 (<https://www.ddg-pharmfac.net/vaxijen/VaxiJen/VaxiJen.html>). Additionally, epitopes with the same amino acid sequence except for the mutation point were used as candidate peptides for variant Omicron.

## 2.7. HLA-A\*02:01 peptide screening in T2 cells

The candidate peptides were synthesized by GenScript Biotechnology Co., Ltd. (Nanjing, China) with a purity > 98 % and suspended in DMSO at a concentration of 10 mmol/L. The titration of peptide concentration was performed as described previously [9]. T2 cells are TAP-deficient T2 cells expressing HLA-A2 molecules on the cell surface. T2 cells were seeded into 96-well plates and then incubated with peptides at a final concentration of 20 μmol/L at 37 °C for 4 h. DMSO was used as a blank control, the reported HLA-A2-restricted influenza A M1 peptide (M58-66 GILGFVFTL) was used as a positive control, and validated Epstein-Barr virus (EBV) peptide (IVTDFSVIK) was used as a negative control [10]. Cells were stained with PE anti-human HLA-A2 antibody (BioLegend, Cat# 343305, US) at 4 °C in the dark for 30 min and acquired in a fluorescence-activated cell sorting (FACS) Canto flow cytometer (BD).

## 2.8. HLA-A2 binding affinity

Ninety-six well U-bottomed plates were coated with 100 μL of 0.5 μg/mL streptavidin (BioLegend, Cat#270302, US) at RT (18–25 °C) for 16–18 h, washed 3 times with washing buffer (BioLegend Cat#421601, US) and blocked with dilution buffer (0.5 mol/L Tris pH 8.0, 1 mol/L NaCl, 1 % BSA, 0.2 % Tween 20) at RT for 30 min. Then, 20 μL of diluted peptide (400 μmol/L) and 20 μL of conditional Flex-T<sup>TM</sup> monomer (200 μg/mL) (BioLegend, Cat#280003, US) were added to 96-well U-bottom plates. To evaluate the outcome of ultraviolet (UV)-mediated HLA peptide exchange, a small aliquot of the exchange reaction mixture 300-fold in 1 × dilution buffer was diluted and kept on ice until usage. DMSO was used as a blank control, influenza A M1 peptide (M58-66 GILGFVFTL) was used as a positive control, and EBV virus peptide (IVTDFSVIK) was used as a negative control. One hundred microliters of specimen were added in duplicate and incubated for 1 h at 37 °C. After washing three times with washing buffer, 100 μL of diluted HRP-conjugated antibodies (BioLegend, Cat#280303, US) were added, incubated for 1 h at 37 °C, and then washed thoroughly. One hundred microliters of substrate solution (10.34 mL DI water, 1.2 mL 0.1 mol/L citric acid monohydrate/trisodium citrate dihydrate, pH 4.0, 240 μL 40 mmol/L ABTS, 120 μL hydrogen peroxide solution) was added and incubated for 8 min at RT in the dark on a plate shaker at 300 × g. The reaction was stopped with 50 μL of stop solution (2 % w/v oxalic acid dihydrate) and read at 414 nm in an Enzyme-linked immunosorbent assay (ELISA) reader within 30 min.

## 2.9. Generation of antigen-specific HLA-A2/A24 tetramer

Thirty microliters of peptide-exchanged HLA-A2/A24 monomer (BioLegend, Cat#280003; 280,019 US) formed in the above steps was mixed with 3.3 μL PE streptavidin (BioLegend Cat#405203, US) on a new plate and incubated on ice in the dark for 30 min. Then, 2.4 μL blocking solution (1.6 μL 50 mmol/L biotin (Thermo Fisher, Cat#B20656, US) plus 198.4 μL phosphate buffer saline (PBS) was added to stop the reaction and incubated at 4–8 °C overnight.

## 2.10. Cell-surface antibodies and tetramer staining and IFN-γ detection of CD8<sup>+</sup> T cells

With the previously reported artificial antigen-presenting cell system from others and our studies, HLA-A2-expressing T2 cells were loaded with peptides for subsequent CD8<sup>+</sup> T cell activation. Briefly, T2 cells were treated with 20 μg/mL mitomycin C for 30 min to stop cell proliferation [11] and loaded with the given epitope peptides for 4 h. Peptide-loaded T2 cells were stained with PE anti-human HLA-A2 antibody (BioLegend, Cat# 343305, US) to analyze the loading rate. CD8<sup>+</sup> T cells were purified from PBMCs with EasySep Human negative selection (Stemcell, Cat# 17953, Canada) with a purity over 95 %. CD8<sup>+</sup> T cells ( $0.25 \times 10^6$ ) isolated from healthy donors were cocultured with  $0.25 \times 10^6$  peptide-loaded T2 cells stained with 5 μmol/L CFSE (TargetMol) and cocultured with 1 μg/mL anti-human CD28 antibodies (BioLegend, Cat# 302901, US) and 50 IU/mL interleukin-2 (IL-2) (SL PHARM, Recombinant Human Interleukin-2 (125Ala) Injection). Then, 50 IU/mL IL-2 and 20 μmol/L mixed peptides were supplemented every two days. On day 3, PBMC specimens were further stained with PE-labeled tetramer (homemade) plus antigen-presenting cell (APC)-labeled human CD8 antibody (BioLegend Cat# 344721, US). On day 7, the rest of cells were restimulated with peptides for 4 h in the presence of Leuko Act Cctl with GolgiPlug (BD, Cat# 550583, US) plus 50 IU/mL IL-2, and the production of interferon (IFN)-γ was checked with PerCP conjugated anti-human IFN-γ (BioLegend, Cat# 502524, US) staining.

## 2.11. ELISpot assays

The thawed PBMCs were rested for 3–4 h in Roswell Park Memorial Institute (RPMI) 1640 medium supplemented with 10 % fetal bovine serum (LONSERA, Uruguay) in a 37 °C incubator. Cells were then stimulated with a 20 μmol/L peptide pool corresponding to ancestral/mutant peptides from B.1.1.529 (Omicron). Cell suspensions were transferred to a Human IFN-γ Precoated ELISPOT Kit (strips) (Dayou, Cat# 2110005) and developed after 3 d according to the manufacturer's instructions. Spots were imaged and counted using an ELISpot reader (Mabtech).

## 2.12. Statistical analysis

The data were analyzed by one-way ANOVA and paired-samples *t* tests for statistical significance by using GraphPad Prism 8 and SPSS 22.0 software. A *P* value less than 0.05 was considered statistically significant.

## 3. Results

### 3.1. Precision HLA typing from RNA sequencing and flow cytometry data

HLA gene cluster plays a crucial role in adaptive immunity and is thus relevant in many biomedical applications. We used OptiType, a novel HLA genotyping algorithm based on integer linear programming, capable of producing accurate predictions from next-generation sequencing (NGS) data not specifically enriched for the HLA cluster (Fig. 1A and B). OptiType significantly outperformed pre-

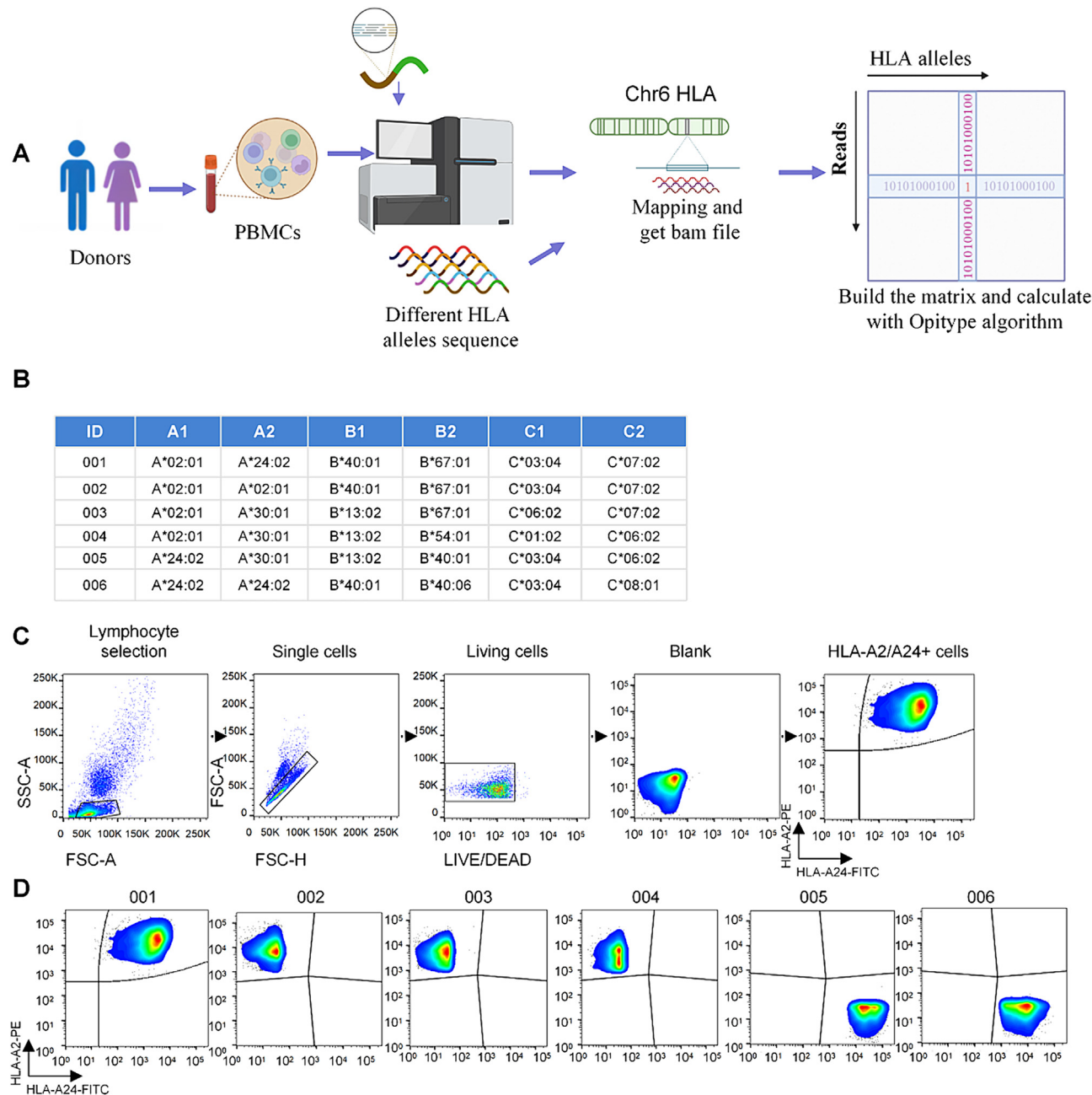


**Fig. 1.** Identification of HLA subtypes. A) OptiType’s four-digit HLA typing pipeline. B) Detailed tables of the HLA-A, B, and C subtypes of all individuals. C) Flow cytometry gating strategy for HLA subtypes. D) PBMCs were isolated by density gradient centrifugation using a lymphocyte separation medium. Representative FACS results of HLA-A2 and HLA-A24 were obtained by flow cytometry. Abbreviations: HLA, human leukocyte antigen; PBMC, peripheral blood mononuclear cell; FACS, fluorescence-activated cell sorting; SSC, side scatter; FSD, front scatter; FITC, fluorescein isothiocyanate.

viously published *in silico* approaches with an overall accuracy of 97 %, enabling its use in a broad range of applications [12]. We also provide an alternative method for the detection of HLA subtypes using the flow cytometry antibodies HLA-A2 and HLA-A24 (Fig. 1C and D). The results showed that HLA subtypes could be identified by RNA sequencing data and flow cytometry.

3.2. Comparison and characterization of SARS-CoV-2 HLA-A2 epitope-specific CD8<sup>+</sup> T cells from COVID-19 vaccination and breakthrough infection donors

We then focused on differences in antigen-specific CD8<sup>+</sup> T cell immune responses after Omicron infection and vaccination by examining the response of CD8<sup>+</sup> T cells to SARS-CoV-2 antigen epitopes in

donors. We recruited 4 HLA-A2 infections (Table S1), 15 individuals who received three doses of inactivated vaccines (Table S2), and 30 breakthrough infections after vaccination (Table S3). In total, 3 pairs of predicted epitopes from the variant strains together with the corresponding epitopes from the ancestral strain were synthesized for MHC-I binding and T-cell activation capability screening. We then focused on the 3 pairs of epitopes with the mutant causing impaired MHC-I binding, which was located in ORF1a, S, and N protein, respectively (Fig. 2A). The T2 binding assay showed decreased MHC-I binding capability by the variant mutated epitopes compared to the corresponding ancestral peptides (Fig. 2B and C). However, these epitopes could still be constructed as peptide-MHC monomers and further tetramers (Fig. 2D). We then constructed 3 pairs of epitope-based tetramers to examine the production of SARS-CoV-2 antigen-specific CD8<sup>+</sup> T



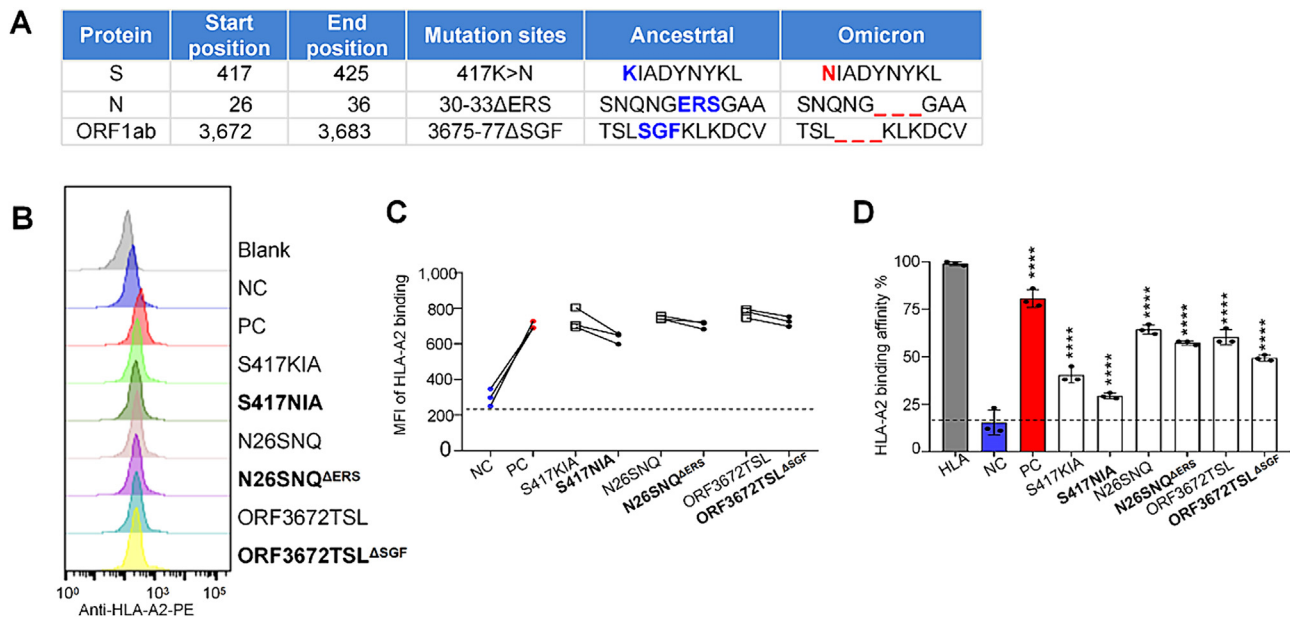


**Fig. 2.** Identification of HLA-A2-restricted T-cell epitopes from the Omicron variant strain. A) Summary of synthesized and validated HLA-A2 epitopes from the Omicron variant strain. B) and C) Comparison of the binding affinity to HLA-A2 of ancestral and mutant epitopes on antigen-presenting T2 cells. Ancestral and mutant epitopes are listed in black and bold, respectively. Paired ancestral and mutant epitopes are listed adjacently. Blank: no peptides; NC: negative control, EBV virus peptide IVTDFSVIK; PC: positive control, influenza A M1 peptide GILGFVFTL. D) Evaluation of ancestral and mutant ancestral and mutant epitope binding to HLA-A2 by ELISA. Data are shown as the mean  $\pm$  SD. The threshold for pMHC formation positivity was set as above the average OD value of the negative control. HLA: control UV-sensitive peptide without UV irradiation. Each dot represents a single individual. \*\*\*\*:  $P < 0.0001$ ; \*\*\*:  $P < 0.001$ ; \*\*:  $P < 0.01$ ; \*:  $P < 0.05$ ; ns: not statistically significant ( $P \geq 0.05$ ). Consistent  $P$  value notations are used throughout the paper. Abbreviations: HLA, human leukocyte antigen; MHC, major histocompatibility complex; SD, standard deviation; UV, ultraviolet; ELISA, enzyme-linked immunosorbent assay; OD, optical density; S, spike protein; N, nucleocapsid; ORF, open reading frame; EBV, Epstein-Barr virus.

cells in subjects (Fig. 3A). Based on tetramer staining, SARS-CoV-2 epitope-specific CD8<sup>+</sup> T cells were detected in most HLA-A2<sup>+</sup> donors (Fig. 3B–G). However, the CD8<sup>+</sup> T cell specificity of all three ancestral epitopes in donor 001 was significantly lower than that of mutant epitopes. The proportion of CD8<sup>+</sup> T-specific cells in donors 002–004 was the opposite (Fig. 3B and C; Fig. S1A). The above results indicated that the CD8<sup>+</sup> T cells specific to the mutant epitope produced by donor 001 may be derived from Omicron infection. The ancestral epitope-specific CD8<sup>+</sup> T cells produced by donors 002–004 may be induced by vaccination. Thus, it can be inferred that donor 001's source of infection may not have come from donors 002–004.

To further analyze whether the CD8<sup>+</sup> T cells specific to volunteers, as distinguished by tetramers, were derived from Omicron infections or vaccination, we recruited individuals who received three doses of the vaccine and those who had breakthrough infections after vaccination. From individuals who received three doses of inactivated vaccine, we observed that the CD8<sup>+</sup> T cell specificity for ancestral epitopes was significantly higher than for mutated epitopes, and the fold change of CD8<sup>+</sup> T cells corresponding to mutated epitopes relative to ancestral epitopes was less than 1 (Fig. 3D and E). However, in individuals who had breakthrough infections after vaccination, the opposite was observed (Fig. 3F and G). In addition, we collected 4 volunteers who received HLA-A2 vaccine and detected the ancestral and mutated epitopes of S 417–425. We analyzed the differences in specific CD8<sup>+</sup> T cell frequencies in the CD3<sup>+</sup>CD8<sup>+</sup> T cell population to verify the reliability of the experimental results, as shown in Fig. S2A and B.

To further validate this hypothesis, we also analyzed the lymphocyte cell responses of the participants by ELISpot. The results showed that donor 001 had cellular immunity induced by Omicron infection, while donors 002–004 had cellular immunity induced by the vaccine (Fig. 4A–C). Our data further suggest that it is possible to distinguish differences in cellular immunity induced by inactivated vaccines and COVID-19 infection by detecting the corresponding epitope-specific CD8<sup>+</sup> T cells.

### 3.3. Comparison and characterization of SARS-CoV-2 HLA-A24 epitope-specific CD8<sup>+</sup> T cells from COVID-19 vaccination and breakthrough infection donors

We recruited 2 HLA-A24 infections (Table S1), and 4 breakthrough infections after vaccination (Table S4). We then constructed 3 pairs of epitope-based tetramers to examine the production of SARS-CoV-2 antigen-specific CD8<sup>+</sup> T cells in subjects (Fig. 5A). Based on tetramer staining, SARS-CoV-2 epitope-specific CD8<sup>+</sup> T cells were detected in most HLA-A24<sup>+</sup> donors (Fig. 5B). The results showed that donor 005 produced no ancestral or mutant-specific CD8<sup>+</sup> T cells, while donor 006 produced significantly more ancestral epitope-specific CD8<sup>+</sup> T cells than mutant epitopes (Fig. 5C). To further analyze whether the CD8<sup>+</sup> T cells specific to volunteers, as distinguished by tetramers, were derived from Omicron infections or vaccination, we recruited individuals who had breakthrough infections after vaccination. In individuals with breakthrough infections after vaccination, we observed that the CD8<sup>+</sup> T cell specificity for mutated epitopes was significantly higher than for wild-type epitopes, and the fold change of CD8<sup>+</sup> T cells corresponding to mutated epitopes relative to ancestral epitopes was greater than 1 (Fig. 5D and E).

To further validate this hypothesis, we also analyzed the lymphocyte cell responses of the participants by ELISpot (Fig. 6A and B) and intracellular IFN- $\gamma$  by flow cytometry (Fig. 6C and D). The results showed that the trend of cellular immunity induced by donors 005 and 006 was consistent with the above results. It can be inferred from the above studies that donor 005 has no cell immunity induced by the vaccine and COVID-19, while donor 006's cell immunity is induced by the vaccine.

## 4. Discussion

The tracking and management of infected persons is one of the important links in the prevention and control of infectious diseases. With the increase of asymptomatic infections, how to identify virus carriers is

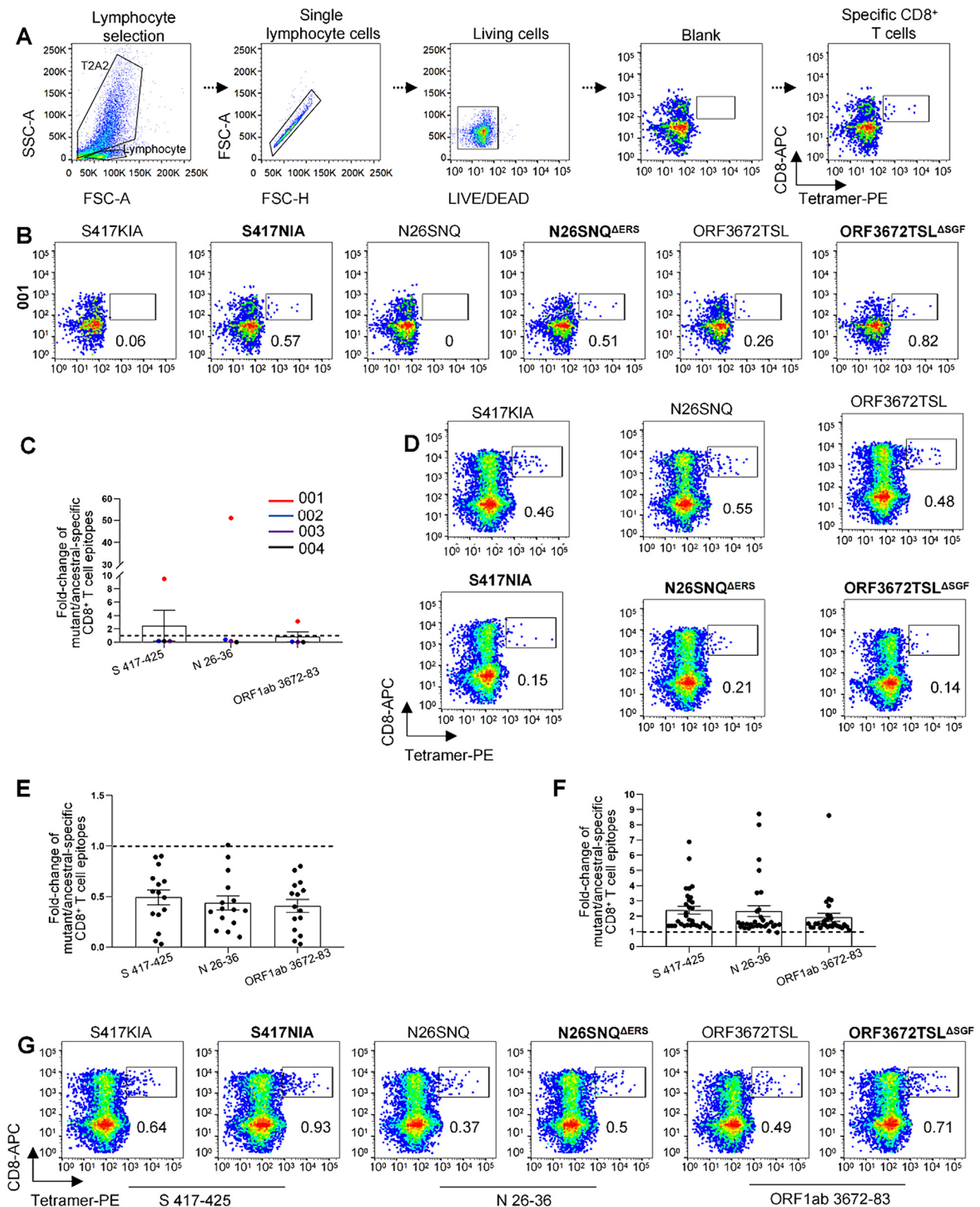
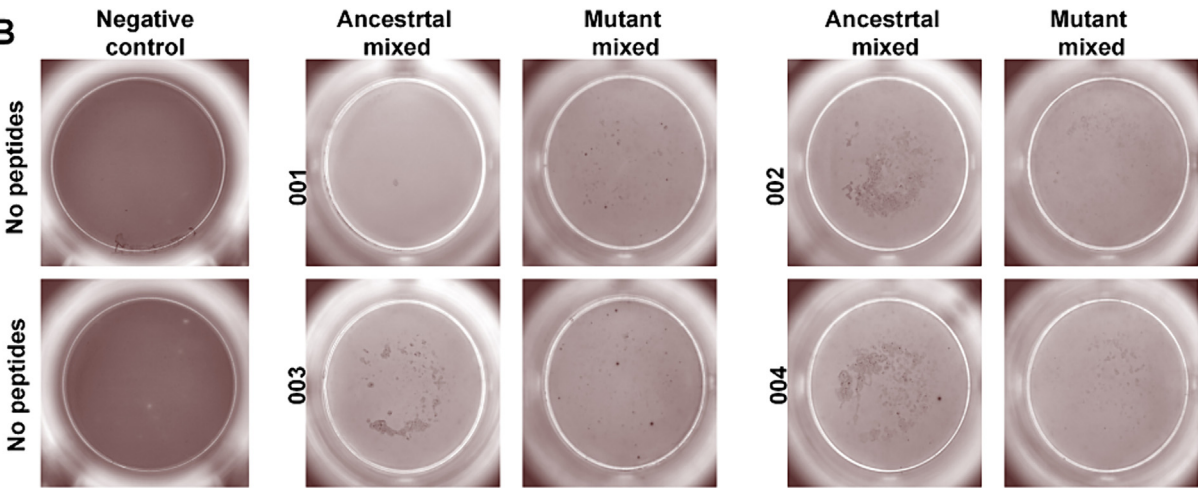


**Fig. 3.** Comparison and characterization of SARS-CoV-2 HLA-A2 epitope-specific CD8<sup>+</sup> T cells from COVID-19 vaccination and breakthrough infection donors. A) Flow cytometry gating strategy for SARS-CoV-2 epitope-specific CD8<sup>+</sup> T cells. B) and C) Representative data for the detection of epitope-specific CD8<sup>+</sup> T cells in HLA-A2<sup>+</sup> donors 001–004 with tetramers prepared using SARS-CoV-2 epitopes. Specific CD8<sup>+</sup> T cells were stained with tetramers prepared using ancestral and mutant SARS-CoV-2 epitopes individually. Overall statistics and comparison of SARS-CoV-2 epitope-specific CD8<sup>+</sup> T cells from 4 donors. D) and E) Representative data for the detection of epitope-specific CD8<sup>+</sup> T cells in HLA-A2<sup>+</sup> COVID-19 vaccination with tetramers prepared using SARS-CoV-2 epitopes. Specific CD8<sup>+</sup> T cells were stained with tetramers prepared using ancestral and mutant SARS-CoV-2 epitopes individually. F) and G) Representative data for the detection of epitope-specific CD8<sup>+</sup> T cells in HLA-A2<sup>+</sup> breakthrough infection donors with tetramers prepared using SARS-CoV-2 epitopes. Specific CD8<sup>+</sup> T cells were stained with tetramers prepared using ancestral and mutant SARS-CoV-2 epitopes individually. Paired ancestral and mutant epitopes are listed adjacently on the x-axis. The specific sequences of the corresponding ancestral and mutant epitopes are shown in Fig. 2A. The flow cytometry gating strategy is shown in Fig. 3A. Abbreviations: HLA, human leukocyte antigen; SARS-CoV-2, severe acute respiratory syndrome coronavirus 2; COVID-19, coronavirus disease 2019; APC, antigen-presenting cell; S, spike protein; N, nucleocapsid; IFN, interferon; ORF, open reading frame

A

ID	Protein	Start position	End position	Mutation sites	Ancestrtal	Omicron
1	ORF1a	3,250	3,261	3255T>I	YQPPQT <b>S</b> ITS	YQPPQ <b>I</b> SITS
2		332	341	339G>D	ITNLCPF <b>G</b> EV	ITNLCPF <b>D</b> EV
3		3,389	3,398	3395P>H	YQCAMR <b>P</b> NFT	YQCAMR <b>H</b> NFT
4		3,673	3,683	3675-77ΔSGF	SL <b>S</b> GFKLKDCV	TSL___KLKDCV
5	S	132	143	142G>D	EFQFCNDPFL <b>G</b> V	EFQFCNDPFL <b>D</b> V
6		417	425	417K>N	<b>K</b> IADYNYKL	<b>N</b> IADYNYKL
7		612	620	614D>G	YQ <b>D</b> VNCTEV	YQ <b>G</b> VNCTEV
8		655	666	655H>Y	<b>H</b> VNNSYECDIPI	<b>Y</b> VNNSYECDIPI
9		964	972	N969N>K	KQLSS <b>N</b> FGA	KQLSS <b>K</b> FGA
10		367	376	371S>L	VLYN <b>S</b> ASFST	VLYN <b>L</b> ASFST
11	M	61	70	63A>T	TL <b>A</b> CFVLA	TL <b>T</b> CFVLA
12	N	8	17	13P>L	NQRN <b>A</b> PRITF	NQRN <b>L</b> PRITF
13		200	208	203R>K	GSS <b>R</b> GTSPA	GSS <b>K</b> GTSPA
14		26	35	30-33ΔERS	SNQNG <b>E</b> RS	SNQNG___GAA
15		200	208	204G>R	GSS <b>R</b> GTSPA	GSS <b>R</b> GTSPA

B



C

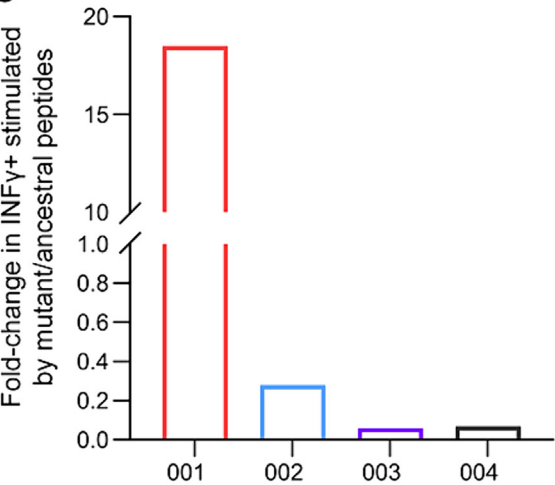


**Fig. 4.** Immune response alteration by HLA-A2 SARS-CoV-2 mutant epitopes. A) Detailed table of Omicron ancestral and mutant epitopes used for ELISpot assays. Exemplary microscopy image (B) and summary statistics (C) for the anti-IFN- $\gamma$  ELISpot assay on lymphocyte cells stimulated by mixed ancestral/mutant SARS-CoV-2 epitopes. They were stimulated with mixed ancestral/mutant peptides cultured for 3 days in precoated anti-IFN- $\gamma$  ELISpot plates. 001-004 represents four donors respectively. The specific sequence of the mixture of ancestral and mutant peptides used is shown in Fig. 4A. Abbreviations: HLA, human leukocyte antigen; SARS-CoV-2, severe acute respiratory syndrome coronavirus 2; S, spike protein; M, membrane protein; N, nucleocapsid; IFN, interferon; ELISpot, enzyme-linked immunosorbent assay; ORF, open reading frame.



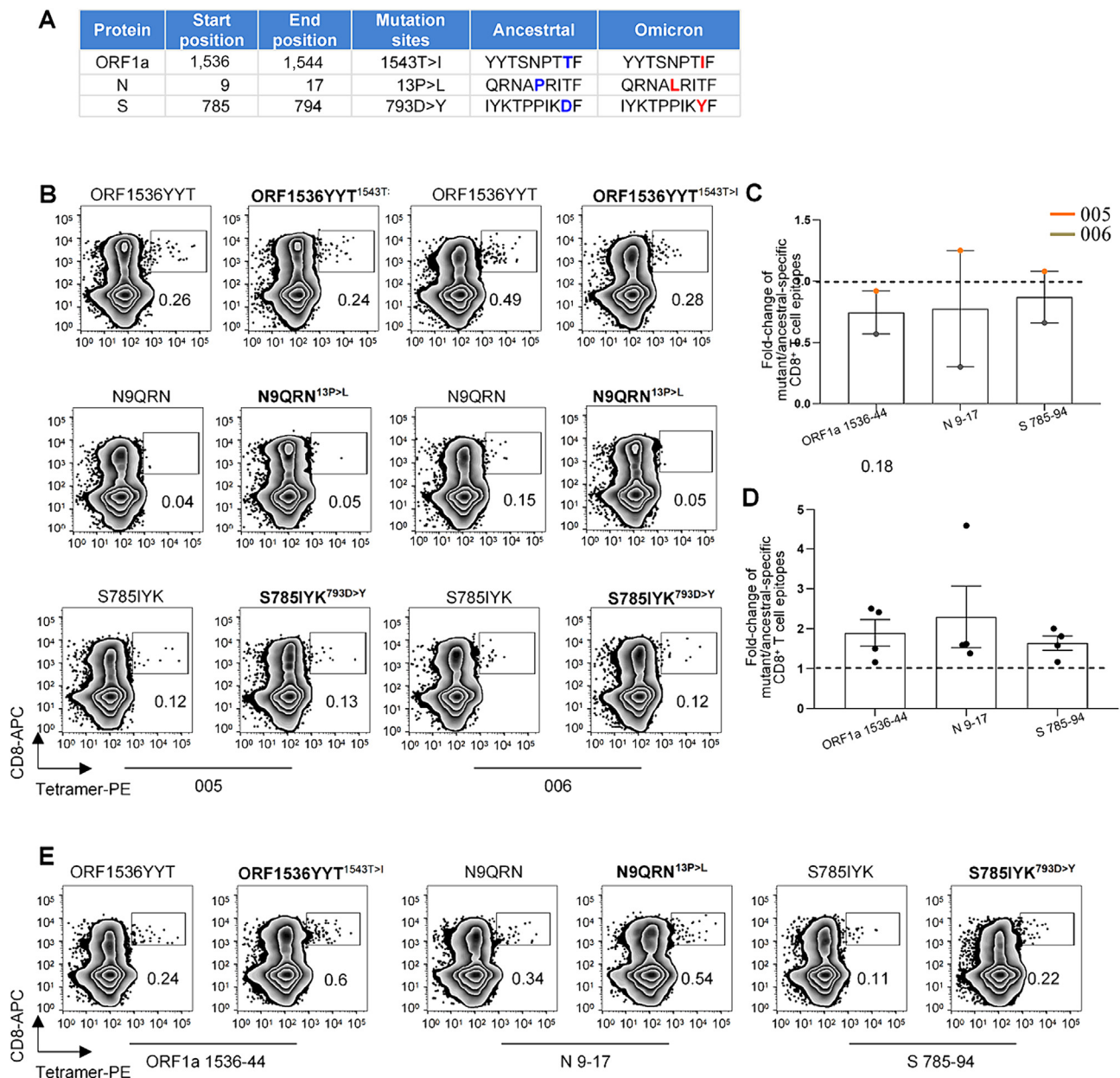


**Fig. 5.** Comparison and characterization of SARS-CoV-2 HLA-A24 epitope-specific CD8<sup>+</sup> T cells from COVID-19 vaccination and breakthrough infection donors. A) Summary of synthesized and validated HLA-A24 epitopes from the Omicron variant strain. B) and C) Representative data for the detection of epitope-specific CD8<sup>+</sup> T cells in HLA-A24<sup>+</sup> donor 005–006 with tetramers prepared using SARS-CoV-2 epitopes. Specific CD8<sup>+</sup> T cells were stained with tetramers prepared using ancestral and mutant SARS-CoV-2 epitopes individually. Overall statistics and comparison of SARS-CoV-2 epitope-specific CD8<sup>+</sup> T cells from 2 donors. D) and E) Representative data for the detection of epitope-specific CD8<sup>+</sup> T cells in HLA-A2<sup>+</sup> + breakthrough infection donors with tetramers prepared using SARS-CoV-2 epitopes. Specific CD8<sup>+</sup> T cells were stained with tetramers prepared using ancestral and mutant SARS-CoV-2 epitopes individually. Paired ancestral and mutant epitopes are listed adjacently on the X-axis. The specific sequences of the corresponding ancestral and mutant epitopes are shown in Fig. 5A. The flow cytometry gating strategy is shown in Fig. 3A. Abbreviations: SARS-CoV-2, severe acute respiratory syndrome coronavirus 2; HLA, human leukocyte antigen; COVID-19, coronavirus disease 2019; S, spike protein; N, nucleocapsid. ORF, Open reading frame.

an urgent problem to be solved. Centers for Disease Control and Prevention (CDC) is tracking and classifying illness in a new way, WGS, using advanced technology to find and stop outbreaks [4]. WGS provides detailed genetic information about the virus, from which it can be inferred that the infected population is infected with the virus subtype, and the source of the virus can be inferred through the evolutionary tree [13]. The results of WGS analysis of the SARS-CoV-2 isolated from the donor 001 confirmed case showed that it was infected with the Omicron BA.2.2. With the reduction of the number of people receiving nucleic acid testing and the increase of asymptomatic infections [14], it is difficult to obtain information on the time of infection in the population,

including the number of infections and virus subtype information over a period of time. Therefore, the neutralizing antibody test for close contacts has become the main method of case traceability detection [15]. Therefore, the detection of neutralizing antibodies in close contacts may become the main method for case tracing detection. However, many studies have shown that there are serious cross-reactions in the detection of neutralizing antibodies between different subtypes, so it is difficult to determine whether a subject is infected or which subtype of the virus is infected by the method of neutralizing antibody detection [9,16].

To this end, we discuss in this study a case-following method for the detection of epitope-specific CD8<sup>+</sup> T cells in the peripheral blood



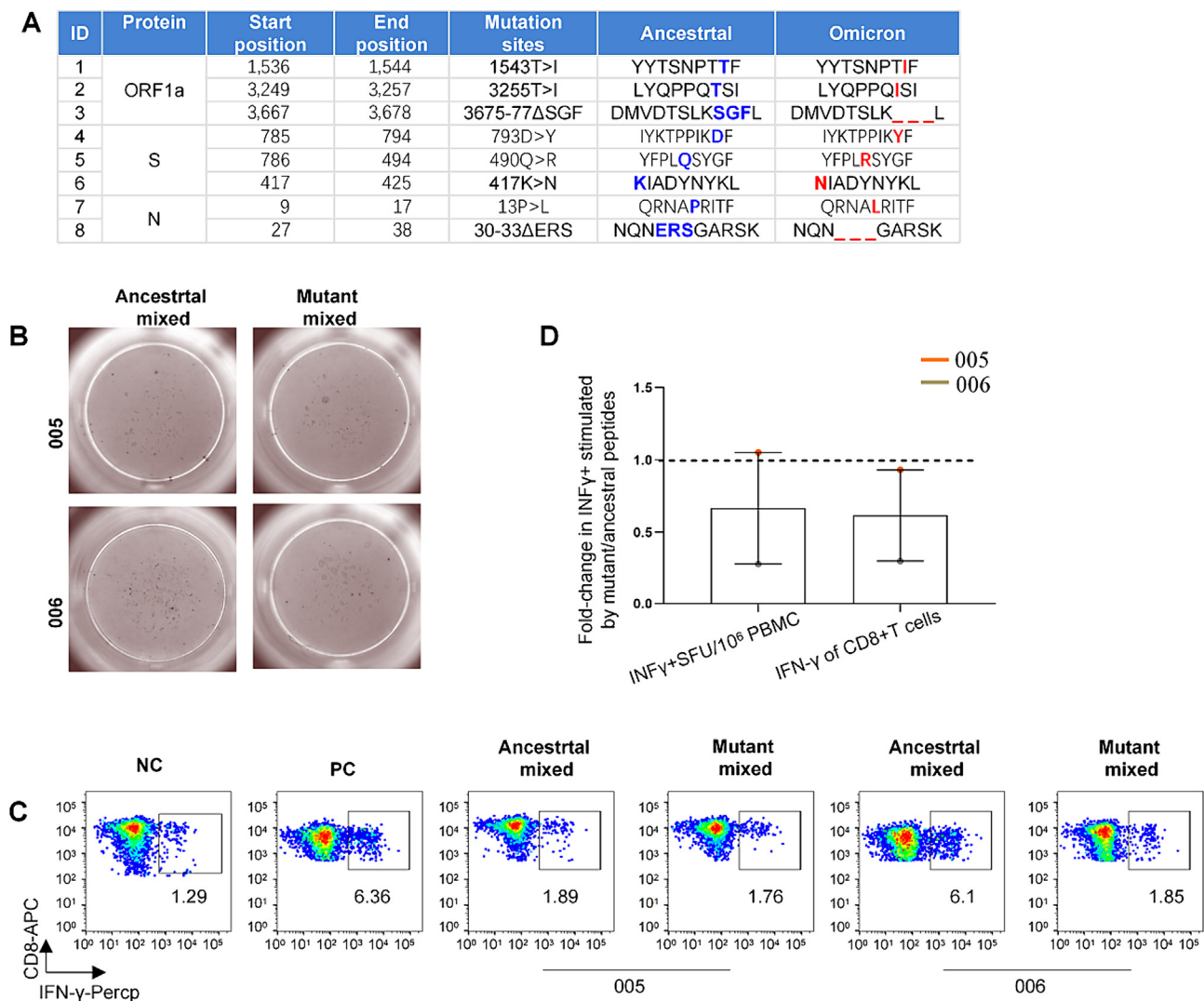


**Fig. 6.** Immune response alteration by HLA-A24 SARS-CoV-2 mutant epitopes. A) Detailed table of Omicron HLA-A24 ancestral and mutant epitopes used for ELISpot assays and intracellular IFN- $\gamma$  flow cytometry. B) Exemplary microscopy image for the anti-IFN- $\gamma$  ELISpot assay on lymphocyte cells stimulated by mixed HLA-A24 ancestral/mutant SARS-CoV-2 epitopes. They were stimulated with mixed ancestral/mutant peptides cultured for 3 days in pre-coated anti-IFN- $\gamma$  ELISpot plates. The specific sequence of the mixture of ancestral and mutant peptides used is shown in Fig. 6A. C) CD8 $^{+}$  T cells isolated from donors were cocultivated with T2 cells loaded with SARS-CoV-2 epitopes at a 1:1 ratio and analyzed for IFN- $\gamma$ . Expression of IFN- $\gamma$  by CD8 $^{+}$  T cells after epitope stimulation for 7 days. The specific sequence of the mixture of ancestral and mutant peptides used is shown in Fig. 6A. D) Overall statistics and comparison of the expression of IFN- $\gamma$  by SARS-CoV-2 epitope-specific CD8 $^{+}$  T cells from 2 donors. NC: negative control, T2 cells loaded with EBV virus peptide IVTDFSVIK; PC: positive control, T2 cells loaded with influenza A M1 peptide GILGFVFTL. Abbreviations: HLA, human leukocyte antigen; SARS-CoV-2, severe acute respiratory syndrome coronavirus 2; IFN, interferon; ELISpot, enzyme-linked immunosorbent assay.

of close contacts. First, the adaptive immune response-mediated anti-SARS-CoV-2 response mainly includes the killing effect of CD8 $^{+}$  T cells on virus-infected cells and the production of specific antibodies by B cells to clear extracellular virus particles [17]. Second, neutralizing antibodies cannot be detected *in vivo* in approximately 10 % of recovered patients, but T-cell immune responses can be detected [18]. Finally, neutralizing antibodies cannot be detected in people who have been vaccinated for more than six months, but antigen-specific T cells can be detected [19–21].

According to the SARS-CoV-2 sequence of case donor 001 (BA.2.2), potential mutant subtype antigen-specific CD8 $^{+}$  T cell epitopes were calculated using the “MHC I Binding” tool (<https://tools.iiedb.org/mhci>). OptiType, a novel HLA genotyping algorithm based on integer linear programming, significantly outperformed previously published *in silico* approaches with an overall accuracy of 97 %. Subsequently, using the artificial APC system, the top 3 BA.HLA-A2 epitope-specific CD8 $^{+}$  T cells were screened out. Four recruited HLA-A2-positive

donors’ BA. HLA-A2 epitope-specific CD8 $^{+}$  T cells were analyzed by tetramer staining flow cytometry. However, since the donor 001 sample had no vaccination history and was infected with BA.2.2 mutant, the results showed that the proportion of epitope-specific CD8 $^{+}$  T cells of the original type was much lower than that of BA.2.2, which was in line with the rheology results. Among the donor 002–004 HLA-A2-positive core close contacts, because they all had a history of vaccination, the proportion of native epitope-specific CD8 $^{+}$  T cells was much higher than that of BA.2.2. Therefore, it is speculated that the donor 002–004 close contacts may not have been infected with BA.2.2. The ELISpot results also showed similar results to tetramer staining flow cytometry. However, due to the small sample size, it is necessary to expand the sample size to further determine whether close contacts have been infected with BA.2.2.

Likewise, we constructed 3 pairs of epitope-based tetramers to examine the generation of SARS-CoV-2 antigen-specific CD8 $^{+}$  T cells in subjects. Based on tetramer staining, it was shown that donor 005

generated no ancestral and mutation-specific CD8<sup>+</sup> T cells, whereas donor 006 generated significantly more ancestral epitope-specific CD8<sup>+</sup> T cells than mutant epitopes. The results of ELISpot and intracellular IFN- $\gamma$  flow staining showed that the tendency of donors 005 and 006 to induce cellular immunity was consistent with the above results. From the above studies, it can be inferred that donor 005 had no vaccine- or COVID-19-induced cellular immunity, while donor 006's cellular immunity was induced by the vaccine.

This study forms a “method for understanding the infection history of SARS-CoV-2 subtypes based on the proportion of epitope-specific CD8<sup>+</sup> T cells in the peripheral blood of subjects”, covering up to 46 % of the population, including 30 % HLA-A2<sup>+</sup> and 16 % HLA-A24<sup>+</sup> donors [22], providing a novel method for SARS-CoV-2 infected case tracing. This method can not only be used in the investigation of the infection history of asymptomatic people but also can be used in the evaluation of the specific cellular immunity level of mutant vaccinees in the future.

### Ethics statement

The study has obtained informed consent from patients and their families to publish their anonymous information in this article. The institutional review board of Jinan University School of Medicine approved the study (JNUKY-2021-009).

### Acknowledgements

This work was supported by the Key Project of Shenzhen Science and Technology Innovation Commission (JCYJ20210324115411030); Natural Science Foundation of China (92169102); R&D Program of Guangzhou Laboratory (SRPG22-006); Sanming Project of Medicine in Shenzhen (SZSM202211023); Guangdong Basic and Applied Basic Research Foundation (2022B1515120043); the Open Project Fund of Guangdong Provincial People's Hospital (YKY-KF202208); National Natural Science Foundation of China (81902097); Funding by Science and Technology Projects in Guangzhou (SL2023A04J01160); the Guangdong Basic and Applied Basic Research Foundation (2023A1515140117); the fellowship of China Postdoctoral Science Foundation (2023TQ0136, 2023M741379); supported by grants from the National Key Research and Development Plan (2023YFE0118700, 2021YFC2301604); the Fundamental Research Funds for the Central Q4 Universities (21623406).

### Conflict of interest statement

The authors declare that there are no conflicts of interest.

### Author contributions

**Congling Qiu:** Investigation, Resources, Writing – original draft. **Bo Peng:** Resources, Software, Data curation. **Chanchan Xiao:** Investigation, Resources, Writing – original draft. **Pengfei Chen:** Investigation. **Lipeng Mao:** Resources, Software, Data curation. **Xiaolu Shi:** Investigation. **Zhen Zhang:** Investigation. **Ziquan Lv:** Investigation. **Qiuying Lv:** Resources. **Xiaomin Zhang:** Resources. **Jiaxin Li:** Resources. **Yanhao Huang:** Resources. **Qinghua Hu:** Writing – original draft. **Guobing Chen:** Conceptualization, Funding acquisition, Writing – review & editing. **Xuan Zou:** Conceptualization, Supervision. **Xiaofeng Liang:** Conceptualization, Funding acquisition, Writing – review & editing.

### Supplementary data

Supplementary data to this article can be found online at <https://doi.org/10.1016/j.bsheat.2024.03.005>.

### References

- [1] E. Han, M.M.J. Tan, E. Turk, D. Sridhar, G.M. Leung, K. Shibuya, N. Asgari, J. Oh, A.L. Garcia-Basteiro, J. Hanefeld, et al., Lessons learnt from easing COVID-19 restrictions: an analysis of countries and regions in Asia Pacific and Europe, *Lancet* 396 (2020) 1525–1534, [https://doi.org/10.1016/s0140-6736\(20\)32007-9](https://doi.org/10.1016/s0140-6736(20)32007-9).
- [2] A.D. Goel, P. Bhardwaj, M. Gupta, N. Kumar, V. Jain, S. Misra, S. Saurabh, M.K. Garg, V.L. Nag, Swift contact tracing can prevent transmission-case report of an early COVID-19 positive case, *J. Infect. Public Health* 14 (2021) 260–262, <https://doi.org/10.1016/j.jiph.2020.12.022>.
- [3] E. Alm, E.K. Broberg, T. Connor, E.B. Hodcroft, A.B. Komissarov, S. Maurer-Stroh, A. Melidou, R.A. Neher, Á. O'Toole, D. Pereyaslov, Geographical and temporal distribution of SARS-CoV-2 clades in the WHO European Region, January to June 2020, *Euro. Surveill.* 25 (2020) 2001410, <https://doi.org/10.2807/1560-7917.es.2020.25.32.2001410>.
- [4] A.H. Løvestad, S.B. Jørgensen, N. Handal, O.H. Ambur, H.V. Aamot, Investigation of intra-hospital SARS-CoV-2 transmission using nanopore whole-genome sequencing, *J. Hosp. Infect.* 111 (2021) 107–116, <https://doi.org/10.1016/j.jhin.2021.02.022>.
- [5] Q. Lei, Y. Li, H. Hou, F. Wang, Z.Q. Ouyang, S.J. Guo, S. Huang, Z. Sun, S. Tao, X. Fan, et al., Antibody dynamics to SARS-CoV-2 in asymptomatic COVID-19 infections, *Allergy* 76 (2021) 551–561, <https://doi.org/10.1111/all.14622>.
- [6] D. Planas, N. Saunders, P. Maes, F. Guivel-Benhassine, C. Planchais, J. Buchrieser, W.H. Bolland, F. Porrot, I. Staropoli, F. Lemoine, et al., Considerable escape of SARS-CoV-2 omicron to antibody neutralization, *Nature* 602 (2022) 671–675, <https://doi.org/10.1038/s41586-021-04389-z>.
- [7] M. Yuan, Y. Wang, H. Lv, T.J.C. Tan, I.A. Wilson, N.C. Wu, Molecular analysis of a public cross-neutralizing antibody response to SARS-CoV-2, *Cell Rep.* 41 (2022), 111650, <https://doi.org/10.1016/j.celrep.2022.111650>.
- [8] J. Deng, J. Pan, M. Qiu, L. Mao, Z. Wang, G. Zhu, L. Gao, J. Su, Y. Hu, O.J. Luo, et al., Identification of HLA-A2 restricted CD8(+) T cell epitopes in SARS-CoV-2 structural proteins, *J. Leukoc. Biol.* 110 (2021) 1171–1180, <https://doi.org/10.1002/jlb.4ma0621-020r>.
- [9] C. Xiao, J. Su, C. Zhang, B. Huang, L. Mao, Z. Ren, W. Bai, H. Li, G. Lei, J. Zheng, et al., Effectiveness of booster doses of the SARS-CoV-2 inactivated vaccine KCONVAC against the mutant strains, *Viruses* 14 (2022) 2016, <https://doi.org/10.3390/v14092016>.
- [10] A. Szolek, B. Schubert, C. Mohr, M. Sturm, M. Feldhahn, O. Kohlbacher, OptiType: precision HLA typing from next-generation sequencing data, *Bioinformatics* 30 (2014) 3310–3316, <https://doi.org/10.1093/bioinformatics/btu548>.
- [11] C. Xiao, C. Qiu, J. Deng, J. Ye, L. Gao, J. Su, O.J. Luo, P. Wang, G. Chen, Optimization of antigen-specific CD8(+) T cell activation conditions for infectious diseases including COVID-19, *StarProtoc.* 2 (2021) 100789, <https://doi.org/10.1016/j.xpro.2021.100789>.
- [12] C. Xiao, L. Mao, Z. Wang, L. Gao, G. Zhu, J. Su, X. Chen, J. Yuan, Y. Hu, Z. Yin, et al., SARS-CoV-2 variant B.1.1.7 caused HLA-A2(+) CD8(+) T cell epitope mutations for impaired cellular immune response, *iScience* 25 (2022) 103934, <https://doi.org/10.1016/j.isci.2022.103934>.
- [13] B. Sobkowiak, K. Kamelian, J.E.A. Zlosnik, J. Tyson, A.G.D. Silva, L.M.N. Hoang, N. Prystajek, C. Colijn, Cov2clusters: genomic clustering of SARS-CoV-2 sequences, *BMC Genomics* 23 (2022) 710, <https://doi.org/10.1186/s12864-022-08936-4>.
- [14] D.P. Oran, E.J. Topol, The proportion of SARS-CoV-2 infections that are asymptomatic, *Ann. Intern. Med.* 174 (2021) 1344–1345, <https://doi.org/10.7326/121-0491>.
- [15] S.C. Taylor, B. Hurst, C.L. Charlton, A. Bailey, J.N. Kanji, M.K. McCarthy, T.E. Morrison, L. Huey, K. Annen, M.G. DomBourian, V. Knight, A new SARS-CoV-2 dual-purpose serology test: highly accurate infection tracing and neutralizing antibody response detection, *J. Clin. Microbiol.* 59 (2021) e02438–e02520, <https://doi.org/10.1128/jcm.02438-20>.
- [16] T. Moyo-Gwete, M. Madzivhandila, Z. Makhado, F. Ayres, D. Mhlanga, B. Oosthuysen, B.E. Lambson, P. Kgagudi, H. Tegally, A. Iranzadeh, et al., Cross-reactive neutralizing antibody responses elicited by SARS-CoV-2 501Y.V2 (B.1.351), *N. Engl. J. Med.* 384 (2021) 2161–2163, <https://doi.org/10.1056/NEJMc2104192>.
- [17] A. Sette, S. Crotty, Adaptive immunity to SARS-CoV-2 and COVID-19, *Cell* 184 (2021) 861–880, <https://doi.org/10.1016/j.cell.2021.01.007>.
- [18] A. Soresina, D. Moratto, M. Chiarini, C. Paolillo, G. Baresi, E. Focà, M. Bezzi, B. Baronio, M. Giacomelli, R. Badolati, Two X-linked agammaglobulinemia patients develop pneumonia as COVID-19 manifestation but recover, *Pediatr. Allergy Immunol.* 31 (2020) 565–569, <https://doi.org/10.1111/pai.13263>.
- [19] I. Schulien, J. Kemming, V. Oberhardt, K. Wild, L.M. Seidel, S. Killmer, F. Sagar, M. S. Daul, A. Lago, H. Decker, et al., Characterization of pre-existing and induced SARS-CoV-2-specific CD8(+) T cells, *Nat. Med.* 27 (2021) 78–85, <https://doi.org/10.1038/s41591-020-01143-2>.
- [20] A. Nelde, T. Bilich, J.S. Heitmann, Y. Maringer, H.R. Salih, M. Roerden, M. Lübke, J. Bauer, J. Rieth, M. Wacker, et al., SARS-CoV-2-derived peptides define heterologous and COVID-19-induced T cell recognition, *Nat. Immunol.* 22 (2021) 74–85, <https://doi.org/10.1038/s41590-020-00808-x>.
- [21] T. Sekine, A. Perez-Potti, O. Rivera-Ballesteros, K. Strålin, J.B. Gorin, A. Olsson, S. Llewellyn-Lacey, H. Kamal, G. Bogdanovic, S. Muschiol, et al., Robust T cell immunity in convalescent individuals with asymptomatic or mild COVID-19, *Cell* 183 (2020) 158–168.e14, <https://doi.org/10.1016/j.cell.2020.08.017>.
- [22] F.F. González-Galarza, L.Y. Takeshita, E.J. Santos, F. Kempson, M.H. Maia, A.L. da Silva, A.L. Teles e Silva, G.S. Ghataoraya, A. Alfievic, A.R. Jones, et al., Allele frequency net 2015 update: new features for HLA epitopes, KIR and disease and HLA adverse drug reaction associations, *Nucl. Acids Res.* 43 (2015) D784–8, <https://doi.org/10.1093/nar/gku1166>.